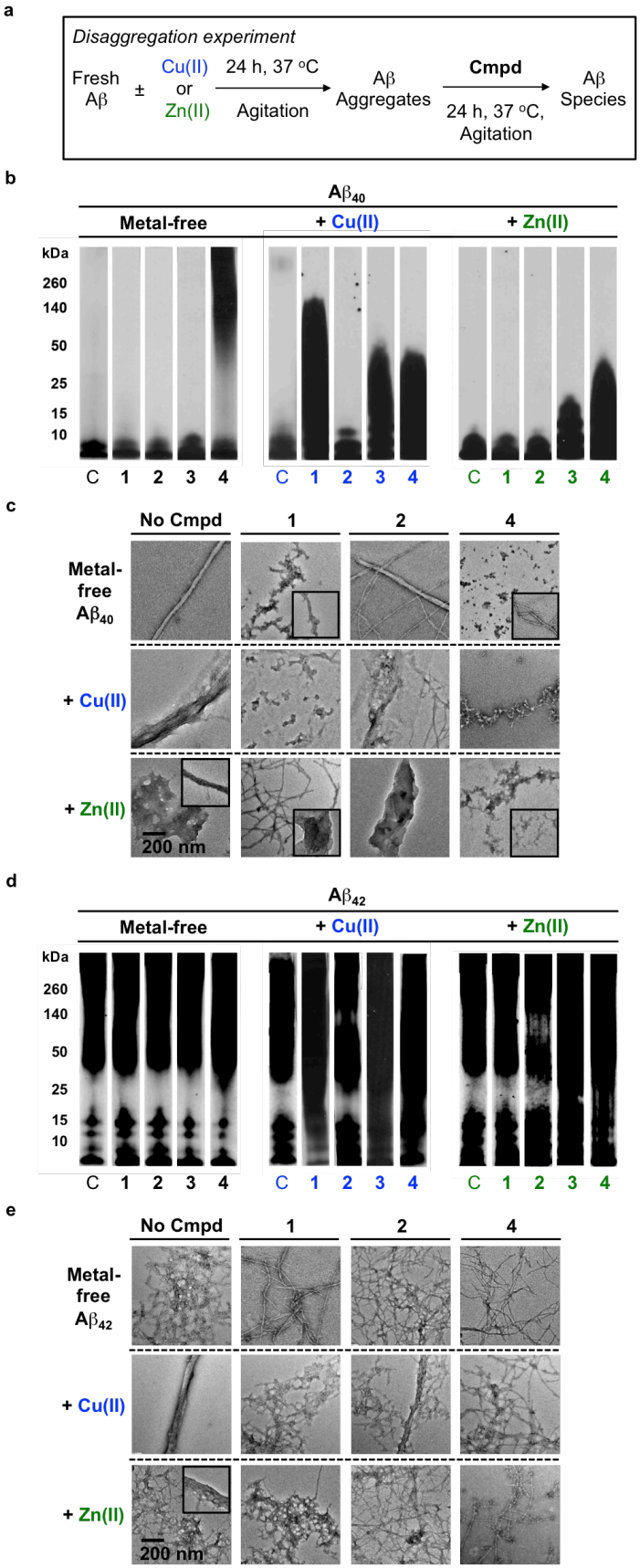
a
Disaggregation experiment
Fresh Aβ
±
Cu(II) or Zn(II)
24 h, 37 °C
Agitation
Aβ Aggregates
Cmpd
24 h, 37 °C, Agitation
Aβ Species
b
Aβ40
Metal-free
+ Cu(II)
+ Zn(II)
kDa
260
140
50
25
15
10
C 1 2 3 4
C 1 2 3 4
C 1 2 3 4
c
No Cmpd
1
2
4
Metal-free Aβ40
+ Cu(II)
+ Zn(II)
200 nm
d
Aβ42
Metal-free
+ Cu(II)
+ Zn(II)
kDa
260
140
50
25
15
10
C 1 2 3 4
C 1 2 3 4
C 1 2 3 4
e
No Cmpd
1
2
4
Metal-free Aβ42
+ Cu(II)
+ Zn(II)
200 nm

Supplementary Figure 1 | Ability of 1-4 to disrupt preformed metal-free and metal–Aβ aggregates. (**a**) Scheme of the disaggregation experiment: Metal-free and metal treated Aβ aggregates were generated by incubating mixtures of freshly prepared $A\beta_{40}$ or $A\beta_{42}$ (25 μM) in the presence or absence of Cu(II) (blue, 25 μM) or Zn(II) (green, 25 μM) at 37 ^{o}C with agitation. After 24 h, the samples were treated with **1**-**4** (50 μM) and incubated for an additional 24 h. Gel electrophoresis and Western blot analysis of the molecular weight distribution of the resulting (**b**) $A\beta_{40}$ and (**d**) $A\beta_{42}$ species using an anti-Aβ antibody (6E10). Morphologies of the (**c**) $A\beta_{40}$ and (**e**) $A\beta_{42}$ species as observed using TEM (scale bar = 200 nm).

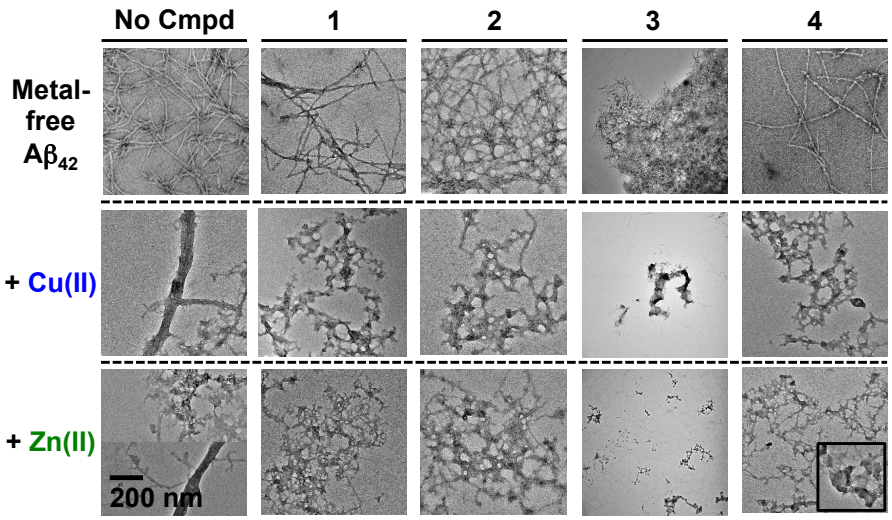

Supplementary Figure 2 | Ability of 1-4 to change the morphology of the resultant $A\beta_{42}$ species from the inhibition experiment (**Fig. 2**). Images were obtained by TEM (scale bar = 200 nm).

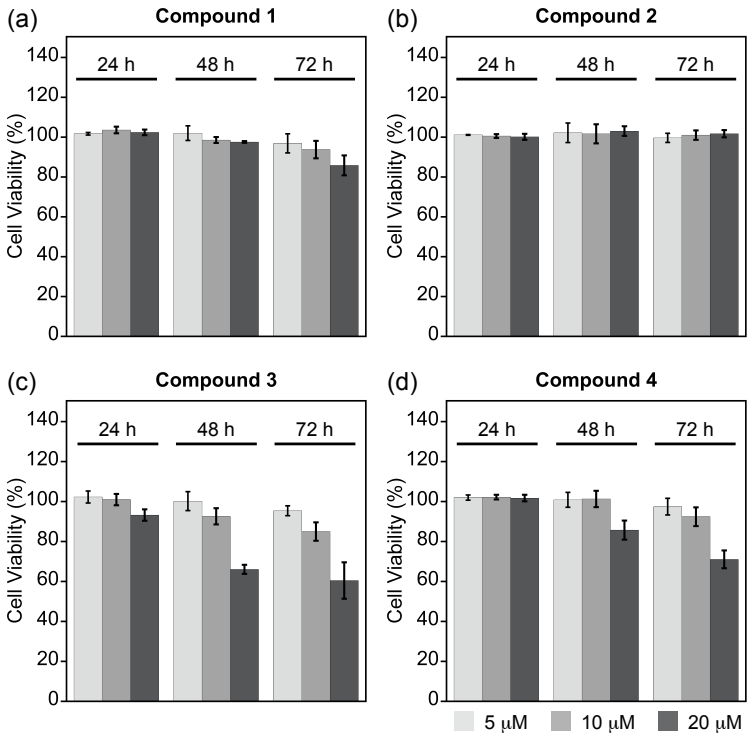

Supplementary Figure 3 | Toxicity of 1-4 at different concentrations (5 to 20 μM) and incubation time points (24 to 72 h) in M17 cells. Viability of cells (%) was calculated relative to that of cells incubated only with 1% v/v DMSO. Error bars represent the standard deviation (s.d.) from three independent experiments ($P < 0.05$).

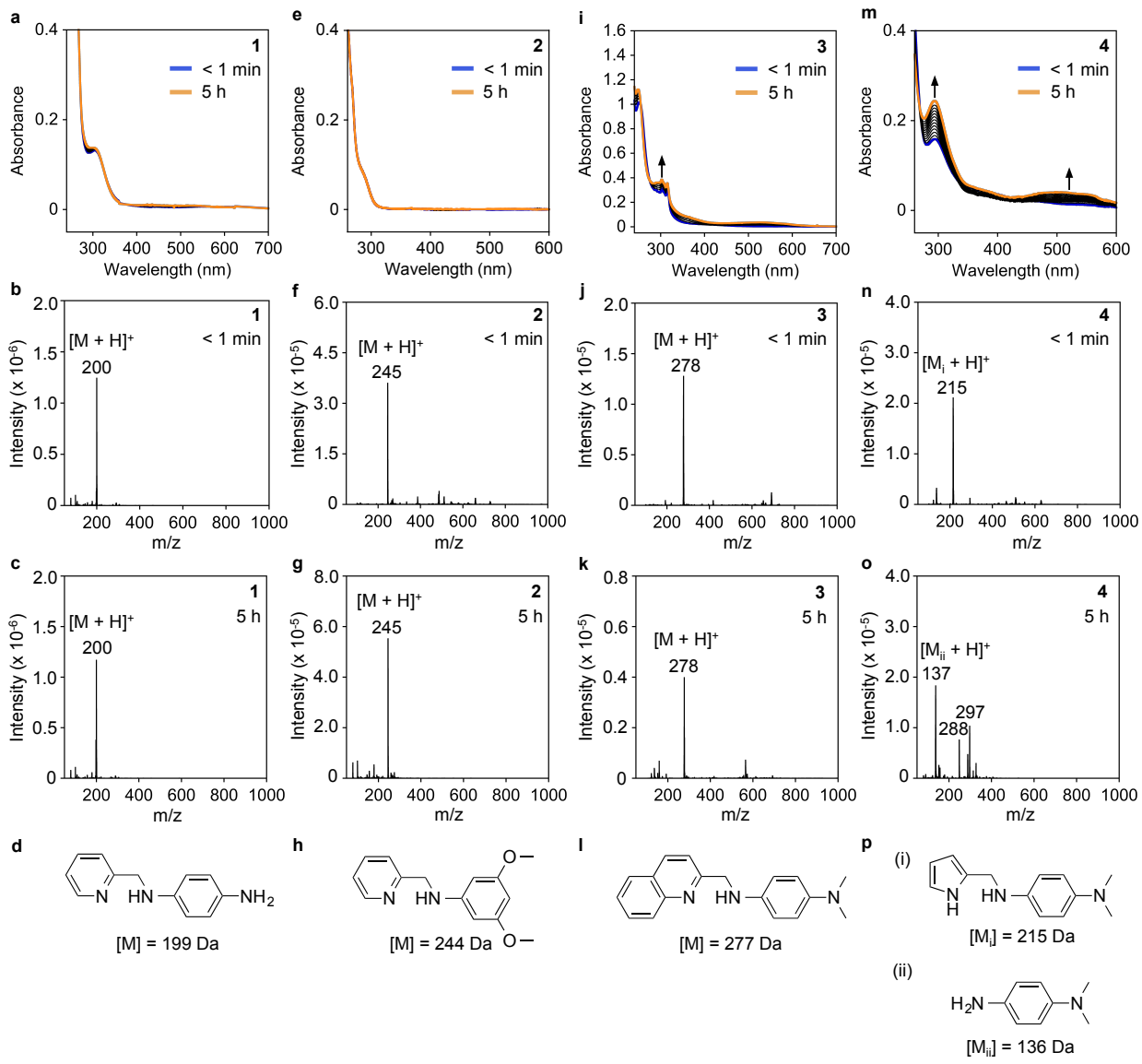

Supplementary Figure 4 | Stability studies of 1-4 in metal-free conditions by UV–Vis and ESI–MS. The stability of **1**-**4** (50 μM) by (**a**,**e**,**i**,**m**) UV-Vis in 20 μM HEPES, pH 7.4, 150 μM NaCl over 5 h (blue: immediately after addition of the sample; orange: after 5 h incubation at 37 °C) and by ESI–MS (**b**,**f**,**j**,**n**) immediately after addition of the sample and (**c**,**g**,**k**,**o**) after incubation at 37 °C for 5 h in ddH_2O. (**d**,**h**,**l**,**p**) Structures and masses of molecules observed in the ESI-MS studies.

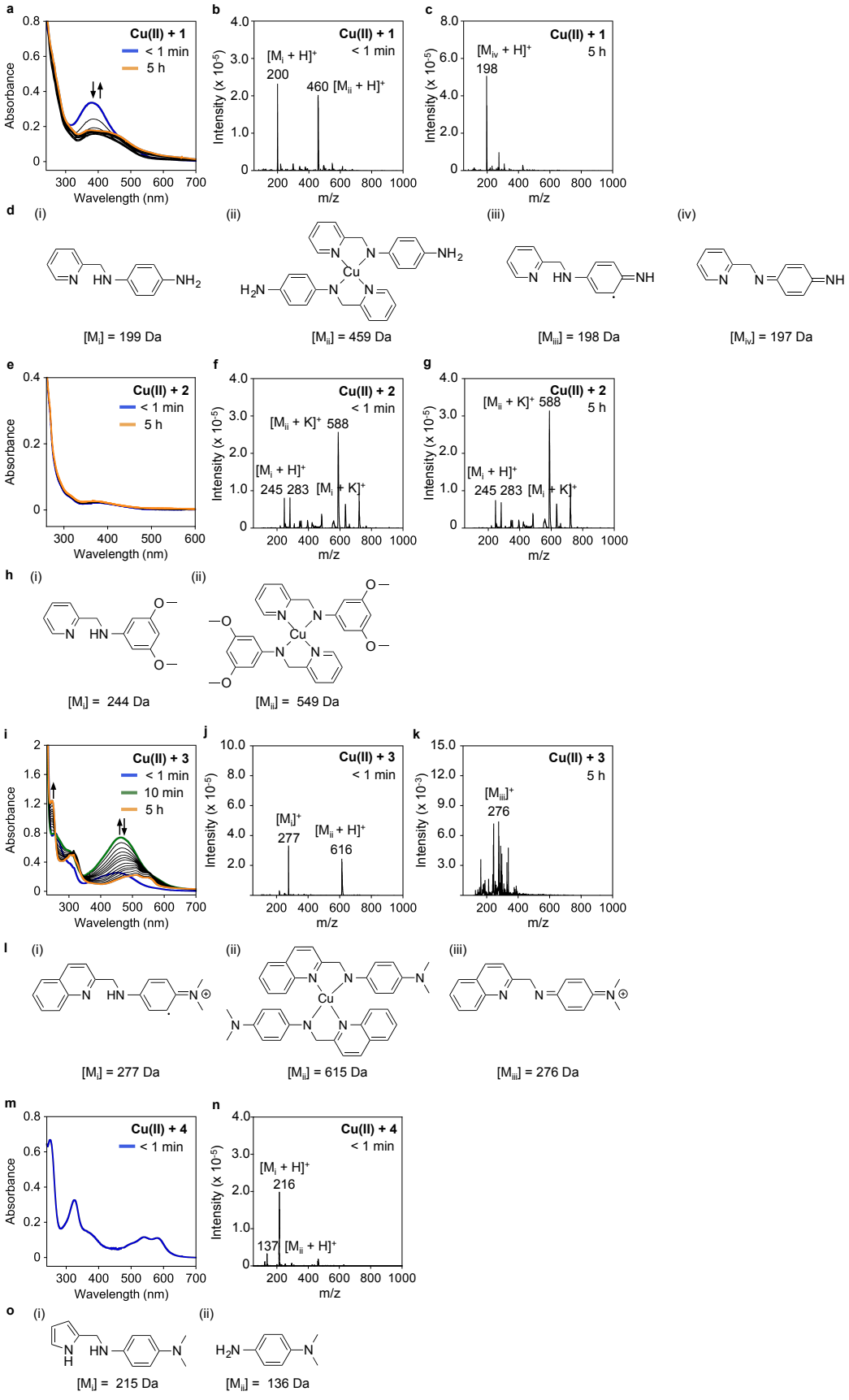
a
Cu(II) + 1
< 1 min
5 h
Absorbance
Wavelength (nm)
b
Cu(II) + 1
< 1 min
[M$_i$ + H]$^+$
200
460 [M$_{ii}$ + H]$^+$
Intensity (x 10^{-5})
m/z
c
Cu(II) + 1
5 h
[M$_{iv}$ + H]$^+$
198
Intensity (x 10^{-5})
m/z
d
(i)
(ii)
(iii)
(iv)
[M$_i$] = 199 Da
[M$_{ii}$] = 459 Da
[M$_{iii}$] = 198 Da
[M$_{iv}$] = 197 Da
e
Cu(II) + 2
< 1 min
5 h
Absorbance
Wavelength (nm)
f
Cu(II) + 2
< 1 min
[M$_{ii}$ + K]$^+$ 588
[M$_i$ + H]$^+$
245 283 [M$_i$ + K]$^+$
Intensity (x 10^{-5})
m/z
g
Cu(II) + 2
5 h
[M$_{ii}$ + K]$^+$ 588
[M$_i$ + H]$^+$
245 283 [M$_i$ + K]$^+$
Intensity (x 10^{-5})
m/z
h
(i)
(ii)
[M$_i$] = 244 Da
[M$_{ii}$] = 549 Da
i
Cu(II) + 3
< 1 min
10 min
5 h
Absorbance
Wavelength (nm)
j
Cu(II) + 3
< 1 min
[M$_i$]$^+$
277
[M$_{ii}$ + H]$^+$
616
Intensity (x 10^{-5})
m/z
k
Cu(II) + 3
5 h
[M$_{iii}$]$^+$
276
Intensity (x 10^{-3})
m/z
l
(i)
(ii)
(iii)
[M$_i$] = 277 Da
[M$_{ii}$] = 615 Da
[M$_{iii}$] = 276 Da
m
Cu(II) + 4
< 1 min
Absorbance
Wavelength (nm)
n
Cu(II) + 4
< 1 min
[M$_i$ + H]$^+$
216
137 [M$_{ii}$ + H]$^+$
Intensity (x 10^{-5})
m/z
o
(i)
(ii)
[M$_i$] = 215 Da
[M$_{ii}$] = 136 Da

Supplementary Figure 5 | Stability studies of 1-4 in the presence of Cu(II) by UV–Vis and ESI–MS. The stability of **1**-**4** (50 μM) in the presence of Cu(II) (25 μM) by (**a**,**e**,**i**,**m**) UV-Vis in 20 μM HEPES, pH 7.4, 150 μM NaCl over 5 h (blue: immediately after addition of the sample; green: after 10 min incubation; orange: after 5 h incubation at 37 ^{o}C) and by ESI–MS (**b**,**f**,**j**,**n**) immediately after addition of the sample and (**c**,**g**,**k**) after incubation at 37 ^{o}C for 5 h in ddH_2O. (**d**,**h**,**l**,**o**) Structures and masses of molecules observed in the ESI-MS studies.

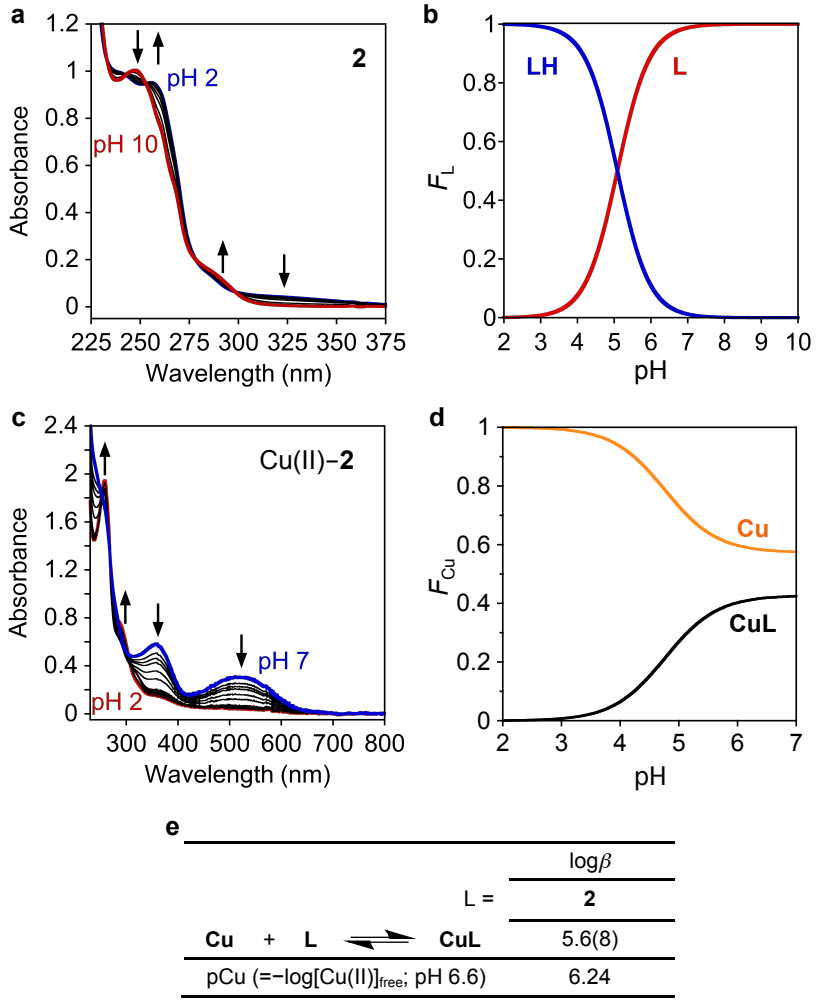

e

					logβ
				L =	**2**
Cu	+	**L**	⇌	**CuL**	5.6(8)
pCu (=−log[Cu(II)]$_{free}$; pH 6.6)					6.24

Supplementary Figure 6 | Solution speciation studies of 2 and Cu(II)–2 complexes. (**a**) Variable-pH UV–Vis titration spectra for **2** (100 μM). The resulting spectra were fitted to obtain the pK_a value [pK_a = 5.0(8)] and the speciation diagram (**b**). F_L = Fraction of ligand with at the specified protonation state. (**c**) Variable-pH UV–Vis titration spectra for Cu(II)–**2**. (**d**,**e**) The speciation diagram (F_{Cu} = Fraction of free Cu and Cu(II)–L) and the stability constants (logβ) of Cu(II)–**2**. The parenthesis indicates the error in the last digit of the values. Conditions: Cu(II):L = 1:2, [**2**] = 50 μM; samples were incubated at room temperature for 24 h before titrations. Charges omitted for clarity.

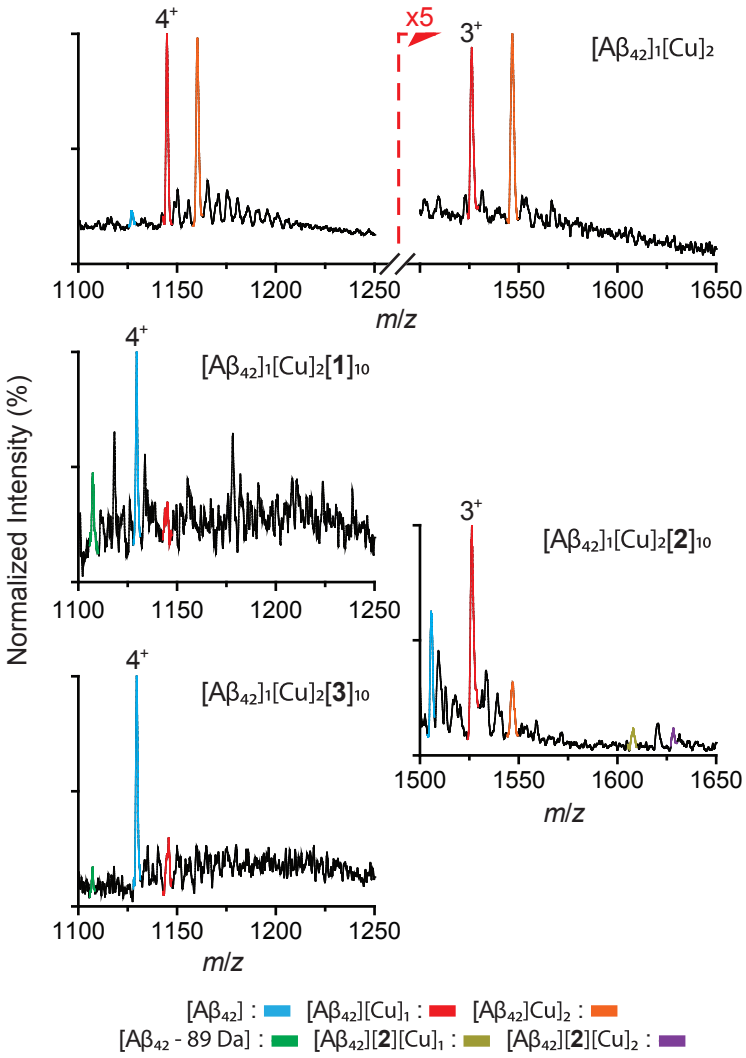

Supplementary Figure 7 | ESI–MS analyses of Aβ$_{42}$ incubated with Cu(II) and 1-3. Compared against metal-containing and ligand-free data, **1**-**3** are shown to be capable of metal-dependent interactions with monomeric Aβ$_{42}$ ([Aβ$_{42}$] = 40 μM; [Cu(II)] = 80 μM; [**1**-**3**] = 400 μM). Both **1** and **3** promote the formation of Aβ mass loss product 89 Da lighter than the metal-free peptide, consistent with our Aβ$_{40}$ data. **2** is observed to produce stable ternary complexes comprising the molecule, Aβ$_{42}$, and one to two Cu(II). Whilst studies with **4** were attempted, the greatly increased aggregation kinetics and additional metal-associated chemical noise provided by the copper ions prevented successful completion. Differences in the charge state depicted in the figure are used to best represent the complexes observed.

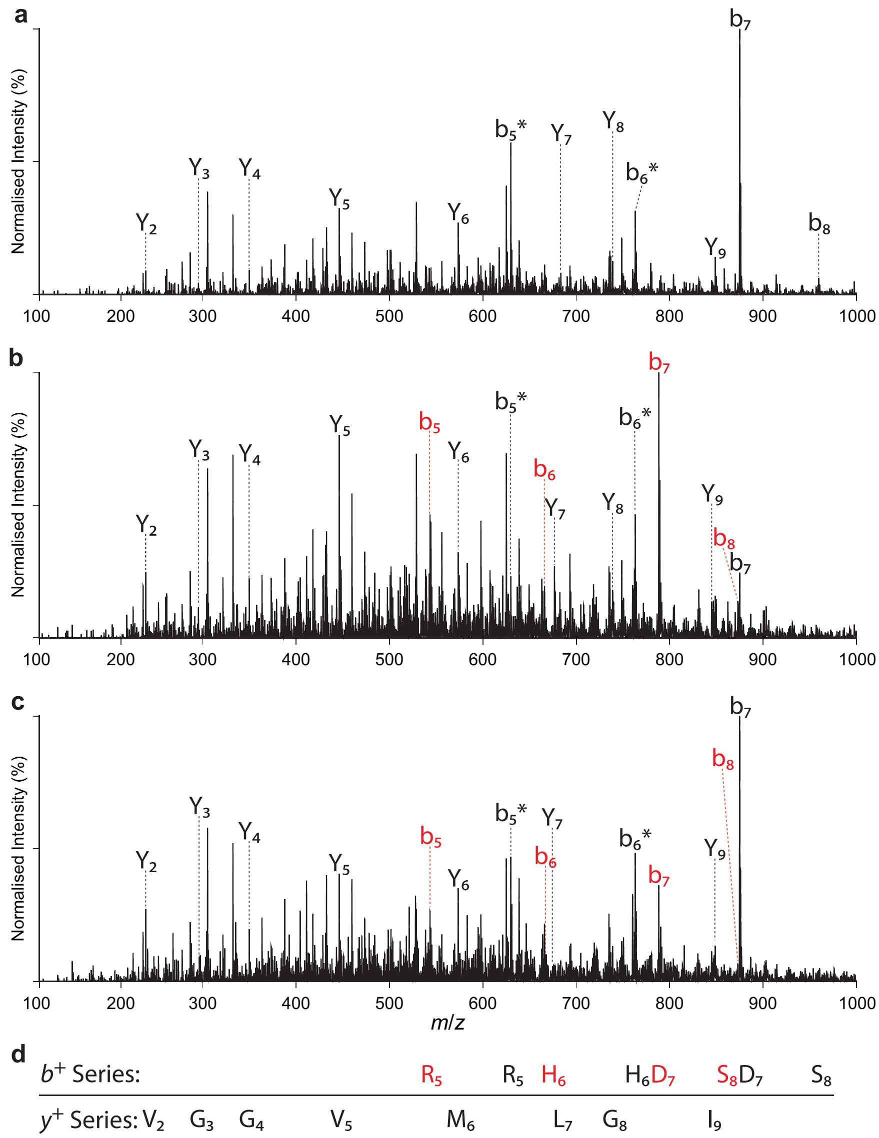

Supplementary Figure 8 | Tandem mass spectrometry sequencing studies of the metal-dependent chemical modification observed in 1 and 3. Tandem mass spectrometry (MS^2) analysis supports that both (**b**) **1** and (**c**) **3** are capable of producing a metal-dependent chemical modification that leads to a mass loss of 89 Da. In both instances data support that the chemical modification is contained within the first five residues of the Aβ N-terminus (D1, A2, E3, F4, and R5), and is consistent with previously published data[1]. Data are shown against control $A\beta_{40}$ MS^2 sequencing data (**a**) acquired under the same conditions. (**d**) Singly charged *b* and *y* ions are shown with the sequence fragments containing the identified mass loss highlighted in red. Ions highlighted with an asterisk indicate overlapping b^+/internal sequence fragments irresolvable due to resolution limitations of the instrument. Complementing the above, a list of all peptides identified in our MS^2 data is presented in Supplementary Table 5.

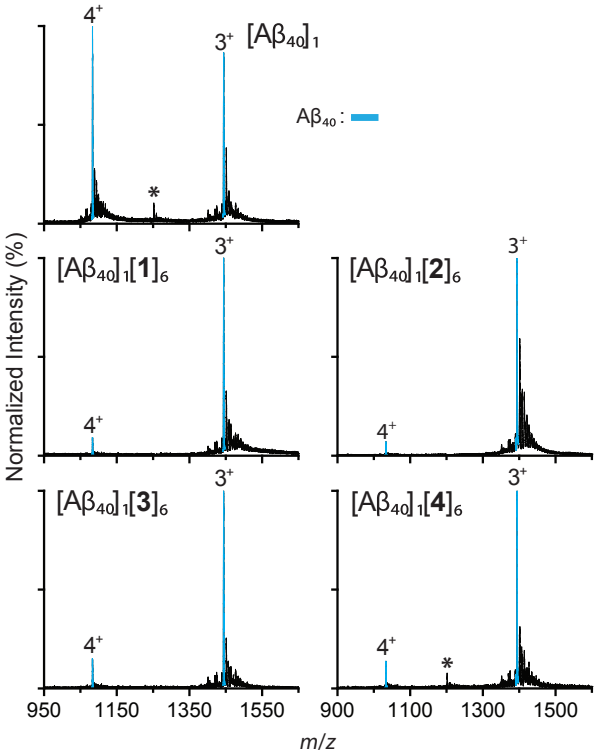

Supplementary Figure 9 | ESI–MS analyses of $A\beta_{40}$ incubated with 1-4 under copper-free conditions. Data support that none of the compounds is capable of binding $A\beta_{40}$ in the absence of Cu(II) within a time frame consistent with those presented in Fig. 5 ([$A\beta_{40}$] = 18 μM; [**1**-**4**] = 120 μM). The * represents an adduct refractory to the preparatory methods employed to prepare the peptides for analysis.

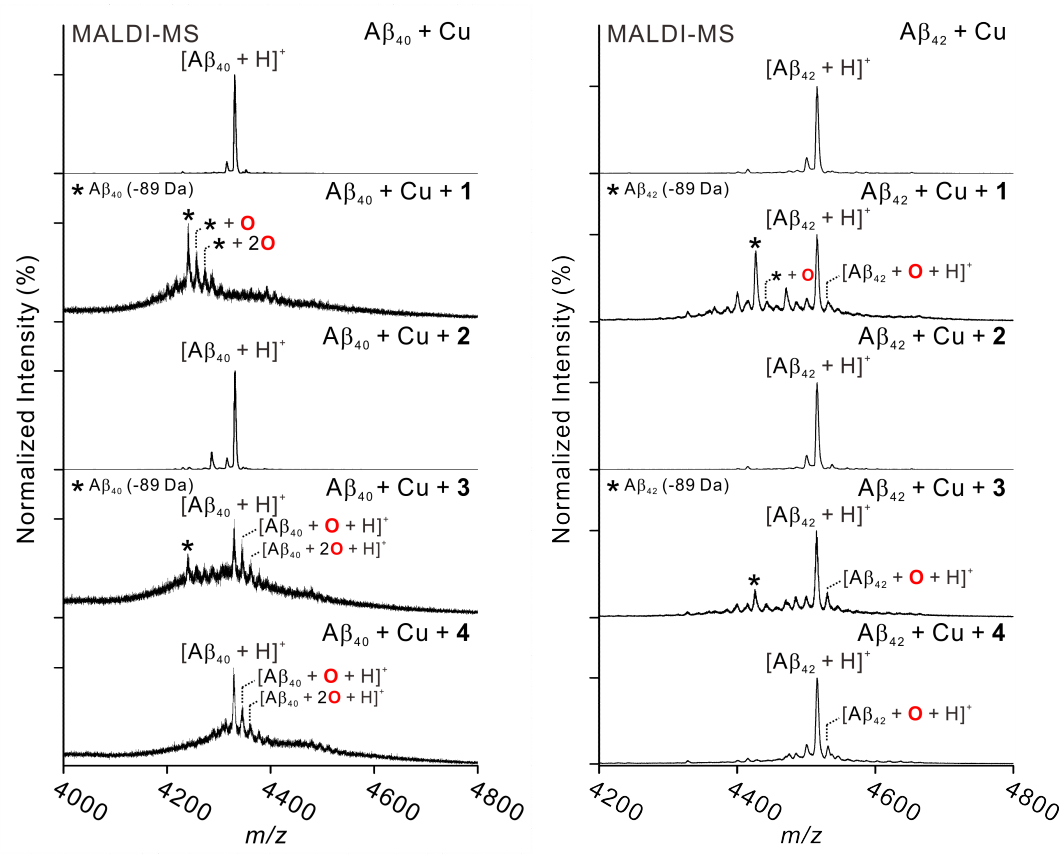

Supplementary Figure 10 | MALDI–MS spectra of $A\beta_{40}$ (left) or $A\beta_{42}$ (right) incubated with 1-4 in the presence of Cu(II) for 24 h. With the addition of **1** and **3**, the truncated $A\beta_{40}$ (loss of 89 Da, indicated with an asterisk) appears, which implies that **1** and **3** have similar interactions to **L2-b** with $A\beta$[1]. Oxidized products were observed in the presence of **1**, **3**, and **4**.

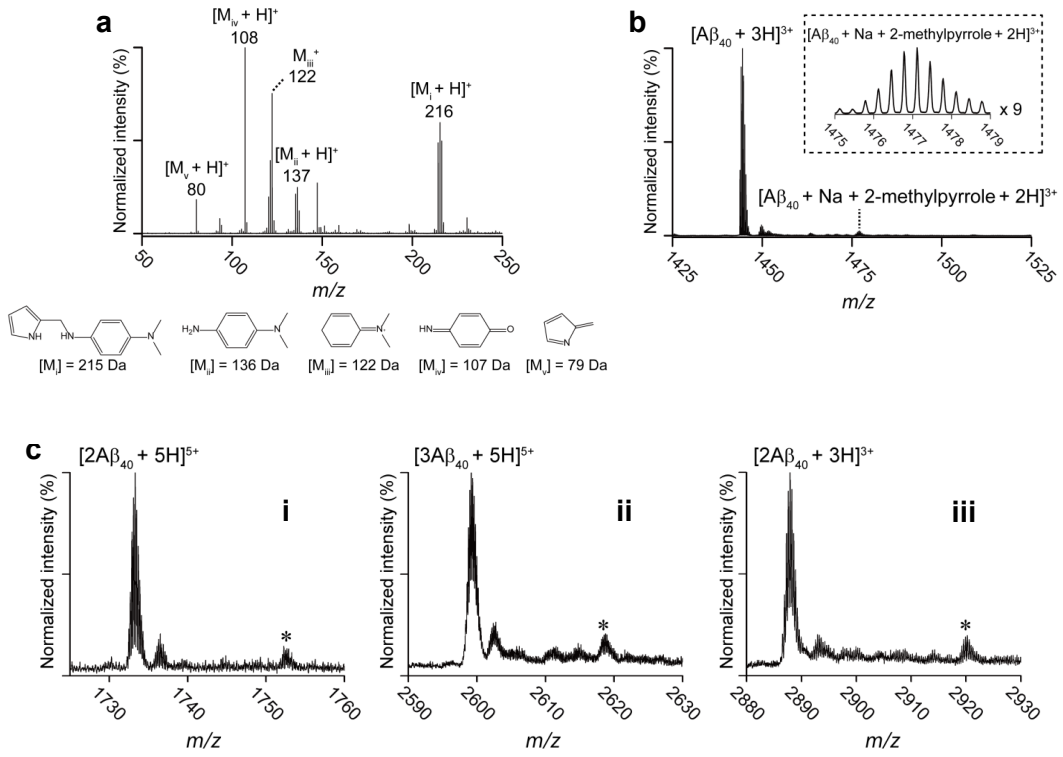

Supplementary Figure 11 | ESI–MS analyses of 4 with Aβ_{40} under metal-free conditions. ESI–MS spectra for analyzing the resultant **4** (**a**; from 50 to 250 Da) and monomeric +3-charged Aβ (**b**; from 1425 to 1525 Da) upon incubation of the compound with Aβ for 6 h. (**a**) **4** is observed to be cleaved into 2-methyl-*1H*-pyrrole (81 Da) and *N,N*-dimethyl-*p*-phenylenediamine (M_{ii}), which could be further transformed into *p*-benzoquinoneimine (M_{iv}). (**b**) The indicated peptide ion has an increase of 103 Da in mass from +3-charged Aβ_{40}, which corresponds to an adduct of Aβ with a sodium ion and 2-methylpyrrole (81 Da). (**c**) ESI–MS spectra for oligomeric Aβ species (**i**, +5-charged dimer; **ii**, +5-charged trimer; **iii**, +3-charged dimer) in the presence of **4**. The asterisk denotes the ion composed of Aβ species, 2-methylpyrrole, and sodium ion [for example, in the case of +5-charged dimer, 2Aβ_{40} + 2-methylpyrrole (81 Da) + Na + 4H].

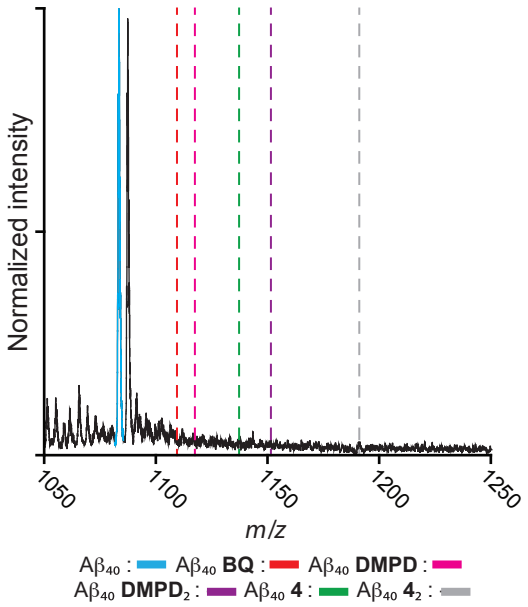

Supplementary Figure 12 | Mass spectrometric analysis of $A\beta_{40}$ incubated with 4 for 24 h. Data shown depict incubations of $A\beta_{40}$ with **4** after 24 h at a ratio of 1:25 (peptide concentration, 25 μM). Data support that an interaction between the ligand and monomeric Aβ was not observed over this time span. Data further account for any potential interactions between Aβ and **DMPD** or benzoquinone (**BQ**). The projected *m*/*z* locations of these peaks are shown using dashed lines.

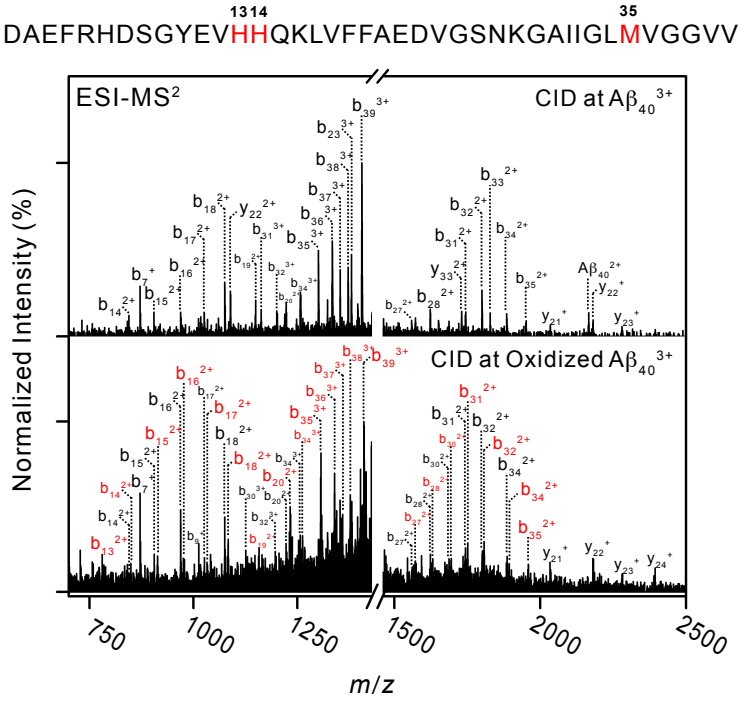

Supplementary Figure 13 | ESI–MS^2 analysis at the +3-charged Aβ (*m/z* 1444) and oxidized Aβ (*m/z* 1449) found in the presence of Cu(II) and 4. b_n^{z+} indicates the *z*-charged N-terminal fragment ions including 1 to n^{th} amino acids. y ions denote the C-terminal fragments. The residue (methionine) is known to be readily oxidized and transformed into the methionine sulfoxide or methionine sulfone[2]. In addition, the histidine residue is another plausible oxidation site in Aβ[3], which can form 2-oxo-histidine[4]. Fragments larger than b_{35} only exist as the oxidized form. From b_{13} to b_{34}, most ions are found in both unoxidized and oxidized forms. These results indicate that there are several oxidation sites other than M35, which are probably H13 and H14.

Supplementary Table 1 | Calculated and measured BBB permeability parameters for 1-4.

Parameters	1	2	3	4	Lipinski's rules and others
MW[a]	199	244	277	215	≤ 450
*c*LogP[b]	1.96	1.73	3.14	1.86	≤ 5.00
HBA[c]	3	4	3	3	≤ 10
HBD[d]	3	1	1	2	≤ 5
PSA (Å^2)[e]	50.9	43.4	28.2	31.1	≤ 90
logBB[f]	−0.563	−0.249	0.191	−0.047	< −1.0 poorly distributed in the brain
$-\log P_e$[g]	5.0(1)	4.2(8)	4.2(2)	4.9(0)	$-\log P_e$ < 5.4 (CNS+); $-\log P_e$ > 5.7 (CNS-)
CNS +/− prediction	CNS+	CNS+	CNS+	CNS+	

[a] MW, molecular weight; [b] *c*logP, calculated log of water–octanol partition coefficient; [c] HBA, hydrogen bond acceptor; [d] HBD, hydrogen bond donor; [e] PSA, polar surface area; [f] logBB = −0.0148 × PSA + 0.152 × *c*logP × 0.130. [g] Determined using the parallel artificial membrane permeability assay adapted for BBB (PAMPA-BBB).

Supplementary Table 2 | Changes in the body weight (gram) of the 5×FAD AD model mice during the experimental period[a].

Gender of animals	Treatment	Day										
		1	3	6	9	12	15	18	21	24	27	30
Male	Vehicle (n = 5)	28.5 ± 0.8*	28.0 ± 0.8	27.0 ± 0.8	27.5 ± 0.8	27.0 ± 0.6	27.8 ± 0.8	27.3 ± 0.8	26.8 ± 0.7	26.8 ± 0.7	27.0 ± 0.7	26.8 ± 0.3
	1 (n = 5)	28.0 ± 0.8	27.6 ± 0.8	27.6 ± 0.8	27.8 ± 0.7	27.4 ± 0.7	27.8 ± 0.7	28.0 ± 0.7	27.8 ± 0.8	27.6 ± 0.7	28.0 ± 0.9	27.0 ± 0.7
	P value	0.6796	0.7265	0.5871	0.7902	0.6596	> 0.9999	0.5340	0.3772	0.4231	0.4103	0.7972
Female	Vehicle (n = 4)	20.3 ± 1.0	20.6 ± 1.0	21.6 ± 0.7	20.6 ± 0.7	20.6 ± 0.7	20.9 ± 1.0	21.6 ± 0.9	21.8 ± 0.6	21.4 ± 0.3	21.3 ± 0.7	21.8 ± 0.3
	1 (n = 5)	20.8 ± 0.6	20.8 ± 0.7	20.8 ± 0.4	21.0 ± 0.6	21.2 ± 0.5	20.8 ± 0.6	21.2 ± 0.8	21.4 ± 0.7	21.4 0.25± 0.7	21.8 ± 0.6	21.6 ± 0.7
	P value	0.6703	0.8703	0.3225	0.6505	0.4958	0.9276	0.7435	0.6860	> 0.9999	0.5983	0.8102

[a] There is no difference in the body weight between vehicle- and **1** (1 mg/kg/day)-treated 5×FAD mice throughout the experimental 30 day period.

*Mean ± s.e.m.

Supplementary Table 3 | Rates of transformation and half lives of 1-4 in the presence and absence of Cu(II).

	Metal-free		+ Cu(II)	
Compound	k (min^{-1})[a]	$t_{1/2}$ (min)[b]	k (min^{-1})[a]	$t_{1/2}$ (min)[b]
1	–[c]	–[e]	0.09 ± 0.03	8 ± 3
2	–[c]	–[e]	–[c]	–[e]
3	–[c]	–[e]	0.013 ± 0.001	53 ± 3
4	0.016 ±0.004	43 ± 5	–[d]	< 1

[a] Rate of decay of the absorbance peak at 250, 384, and 400 nm for **4**, [Cu(II) + **1**], and [Cu(II) + **2**], respectfully. [b] Half life of the absorbance peak in minutes. [c] Spectral changes were too slow to accurately measure the rate during the duration of the experiment. [d] Decay of compound occurred too rapidly to measure in the experiment conditions ([**1-4**] = 50 μM; [Cu] = 25 μM; 25 μM HEPES, pH 7.4, 150 μM NaCl; 37 °C). [e] No noticeable spectral changes were observed over 5 h.

Supplementary Table 4 | Calculated collision cross section (CCS) from IM–MS analysis.

	Conformational Species (Å^2)									
	1		2		3		4		5	
$A\beta_{40}$	658.6	+/- 30.6	721.8	+/- 31.4	X		X		X	
$A\beta_{40}$ Cu	658.7	+/- 28.8	727.3	+/- 31.6	782.3	+/- 34.7	X		X	
$A\beta_{40}$ Cu_2	656.9	+/- 32.5	732.8	+/- 31.9	786.4	+/- 35.6	X		X	
$A\beta_{40}$ **2** Cu	X		717.1	+/- 31.3	X		682.9	+/- 32.5	760.3	+/- 33.0
$A\beta_{40}$ **2** Cu_2	X		X		X		683.7	+/- 36.3	761.2	+/- 40.8

Calculated CCS data are given for the presented stoichiometries and have been calculated using established methods[5,6]. These data suggest the existence of five different conformational species across all ligand stoichiometries observed. Two of these are observed only with **2**. Data are the average of six repeats with errors reported as a function of least square analysis.

Supplementary Table 5. Products of collision induced fragmentation identified.

Products of collision induced dissociation	Ion species observed				
b sequence ions	z	*m*/*z*	Apo	Derivative 1 modification	Derivative 3 modification
b_4	1	463.1823	No	No	No
$b_5^{\ddagger}$	1	619.2835	Yes	No	Yes
b_6^{*}	1	756.3424	Yes	Yes	Yes
b_7	1	871.3693	Yes	Yes	Yes
b_8	1	958.4013	Yes	No	No
b_9	1	1015.4228	Yes	No	No
b_{10}	1	1178.4861	Yes	No	No
b_{11}	1	1307.5287	Yes	No	Yes
b_{12}	1	1406.5971	No	No	No
b_8	2	479.7043	No	No	No
b_9	2	508.215	Yes	No	No
b_{10}	2	589.7467	No	No	No
b_{11}	2	654.268	Yes	No	Yes
b_{12}	2	703.8022	Yes	Yes	Yes
b_{13}	2	772.3317	Yes	No	Yes
b_{14}	2	840.8611	Yes	No	Yes
b_{15}	2	904.8904	Yes	No	Yes
b_{16}	2	968.9379	Yes	No	Yes
b_{17}	2	1025.4799	Yes	No	Yes
b_{18}	2	1075.0141	Yes	No	Yes
b_{19}	2	1148.5483	Yes	No	Yes
b_{20}	2	1222.0825	Yes	No	Yes
b_{21}	2	1257.6011	Yes	No	Yes
b_{22}	2	1322.1224	Yes	No	Yes
b_{23}	2	1379.6359	Yes	Yes	Yes
b_{24}	2	1429.1701	Yes	No	Yes
b_{25}	2	1457.6808	Yes	Yes	Yes
b_{26}	2	1501.1968	Yes	No	No
b_{27}	2	1558.2183	Yes	No	No
b_{28}	2	1622.2658	Yes	No	No
b_{29}	2	1650.7765	No	No	No
b_{30}	2	1686.2951	No	No	No
b_{31}	2	1742.8371	Yes	No	No
b_{32}	2	1799.3791	Yes	No	No
b_{33}	2	1827.8898	No	No	No

b_{34}	2	1884.4319	Yes	No	No
b_{35}	2	1949.9521	No	No	No
b_{26}	3	1001.1336	Yes	No	No
b_{27}	3	1039.1479	Yes	No	No
b_{28}	3	1081.8463	Yes	No	No
b_{29}	3	1100.8534	Yes	No	No
b_{30}	3	1124.5325	Yes	No	No
b_{31}	3	1162.2271	Yes	No	No
b_{32}	3	1199.9218	Yes	No	No
b_{33}	3	1218.929	Yes	No	No
b_{34}	3	1256.6237	Yes	No	No
b_{35}	3	1300.3038	Yes	No	No
b_{36}	3	1333.3266	Yes	No	No
b_{37}	3	1352.3338	Yes	No	No
b_{38}	3	1371.341	Yes	No	No
b_{39}	3	1404.3638	Yes	No	No
Modified b_4	1	374.1261	No	No	No
Modified b_5	1	530.2272	No	Yes	Yes
Modified b_6	1	667.2861	No	Yes	Yes
Modified b_7	1	782.3131	No	Yes	Yes
Modified b_8	1	869.3451	No	Yes	Yes
Modified b_9	1	926.3666	No	No	No
Modified b_{11}	2	609.7399	No	Yes	Yes
Modified b_{12}	2	659.2741	No	Yes	No
Modified b_{13}	2	727.8035	No	Yes	Yes
Modified b_{14}	2	796.333	No	Yes	Yes
Modified b_{15}	2	860.3623	No	Yes	Yes
Modified b_{16}	2	924.4098	No	Yes	Yes
Modified b_{17}	2	980.9518	No	Yes	Yes
Modified b_{18}	2	1030.486	No	Yes	Yes
Modified b_{19}	2	1104.0202	No	Yes	Yes
Modified b_{20}	2	1177.5544	No	Yes	Yes
Modified b_{21}	2	1213.073	No	Yes	Yes
Modified b_{22}	2	1277.5943	No	Yes	No
Modified b_{23}	2	1335.1077	No	Yes	Yes
Modified b_{24}	2	1384.642	No	Yes	No
Modified b_{25}	2	1413.1527	No	Yes	Yes
Modified b_{26}	2	1456.6687	No	No	No
Modified b_{27}	2	1513.6902	No	Yes	No
Modified b_{28}	2	1577.7376	No	Yes	No
Modified b_{29}	2	1606.2484	No	No	No

Modified b_{30}	2	1641.7669	No	Yes	Yes
Modified b_{31}	2	1698.309	No	Yes	Yes
Modified b_{32}	2	1754.851	No	No	No
Modified b_{33}	2	1783.3617	No	Yes	No
Modified b_{34}	2	1839.9038	No	Yes	Yes
Modified b_{27}	3	1009.4625	No	No	No
Modified b_{28}	3	1052.1609	No	Yes	No
Modified b_{29}	3	1071.168	No	Yes	Yes
Modified b_{30}	3	1094.847	No	Yes	Yes
Modified b_{31}	3	1132.5417	No	Yes	Yes
Modified b_{32}	3	1170.2364	No	Yes	Yes
Modified b_{33}	3	1189.2436	No	Yes	Yes
Modified b_{34}	3	1226.9383	No	Yes	Yes
Modified b_{35}	3	1270.6184	No	Yes	Yes
Modified b_{36}	3	1303.6412	No	Yes	Yes
Modified b_{37}	3	1322.6484	No	No	No
Modified b_{38}	3	1341.6555	No	Yes	Yes
Modified b_{39}	3	1374.6783	No	Yes	Yes

Products of collision induced dissociation	Ion species observed				
y sequence ions	z	*m*/*z*	Apo	Derivative 1 modification	Derivative 3 modification
y_2	1	217.1547	Yes	Yes	Yes
y_3	1	274.1761	Yes	Yes	Yes
y_4	1	331.1976	Yes	Yes	Yes
y_5	1	430.266	Yes	Yes	Yes
y_6	1	561.3065	Yes	Yes	Yes
y_7	1	674.3906	Yes	Yes	Yes
y_8	1	731.412	Yes	Yes	Yes
y_9	1	844.4961	Yes	Yes	Yes
y_{10}	1	957.5802	No	No	No
y_{20}	2	943.5062	No	No	No
y_{21}	2	1017.0404	Yes	Yes	Yes
y_{22}	2	1090.5746	No	Yes	Yes
y_{23}	2	1140.1088	No	No	No
y_{31}	2	1657.3737	No	No	No
y_{32}	2	1685.8845	Yes	Yes	Yes
y_{33}	2	1729.4005	Yes	Yes	Yes
y_{34}	2	1786.9139	Yes	Yes	Yes

y_{35}	2	1855.4434	Yes	No	No
y_{36}	2	1933.494	No	No	No
y_{31}	3	1105.2516	No	No	No
y_{32}	3	1124.2587	Yes	Yes	Yes
y_{33}	3	1153.2694	Yes	No	No
y_{34}	3	1191.6117	Yes	No	No
y_{35}	3	1237.298	No	No	No

Products of collision induced dissociation	Ion species observed				
Internal sequence ions	z	*m*/*z*	Apo	Derivative 1 modification	Derivative 3 modification
KGA-NH3 and QK-NH3	1	240.1343	Yes	Yes	Yes
KGA and QK	1	257.1608	Yes	Yes	Yes
HQ	1	266.1248	Yes	Yes	Yes
VGGV-28	1	285.1921	Yes	Yes	Yes
GLM	1	302.1533	Yes	Yes	Yes
VGGV	1	313.187	Yes	Yes	Yes
MVGG	1	345.1591	Yes	Yes	Yes
AIIG and GAII	1	355.234	Yes	Yes	Yes
KGAI and QKL	1	370.2449	Yes	Yes	Yes
GSNK and SNKG	1	387.1987	No	Yes	Yes
VFF	1	394.2125	Yes	Yes	Yes
HQF	1	394.2197	Yes	Yes	Yes
GLMV and LMVG	1	401.2217	Yes	Yes	Yes
GAIIG	1	412.2554	Yes	Yes	Yes
GSNKG-28	1	416.2252	Yes	Yes	Yes
MVGGV-28	1	416.2326	Yes	Yes	Yes
GSNKG	1	444.2201	Yes	Yes	Yes
MVGGV	1	444.2275	Yes	Yes	Yes
QKLV-NH_3	1	452.2867	Yes	Yes	Yes
VGSNK-28	1	458.2722	Yes	Yes	Yes
KGAII	1	483.3289	Yes	Yes	Yes
NKGAI	1	484.2878	No	No	Yes
VGSNK	1	486.2671	Yes	Yes	Yes
GAIIGL-28	1	497.3446	Yes	Yes	Yes
HQKL	1	507.3038	Yes	Yes	Yes
IGLMV	1	514.3058	No	No	Yes
GSNKGA	1	515.2572	Yes	Yes	Yes
GLMVGG	1	515.2646	Yes	Yes	Yes

GAIIGL	1	525.3395	Yes	Yes	Yes
SNKGAI-28	1	543.3249	Yes	Yes	Yes
IGLMVG-28	1	543.3323	Yes	Yes	Yes
SNKGAI	1	571.3198	Yes	Yes	Yes
IGLMVG	1	571.3272	Yes	Yes	Yes
VGSNKGA-28	1	586.3307	Yes	Yes	Yes
GLMVGGV-28	1	586.3381	Yes	Yes	Yes
FAEDVG-28	1	591.2773	Yes	Yes	Yes
HQKLV	1	606.3722	Yes	Yes	Yes
VGSNKGA	1	614.3257	Yes	Yes	Yes
GLMVGGV	1	614.333	Yes	Yes	Yes
FAEDVG‡	1	619.2722	Yes	Yes	Yes
GSNKGAI	1	628.3413	Yes	Yes	Yes
IGLMVGG	1	628.3487	Yes	Yes	Yes
GAIIGLM	1	656.38	Yes	Yes	Yes
IIGLMVG	1	684.4113	Yes	Yes	Yes
VGSNKGAI-28	1	699.4148	Yes	Yes	Yes
IGLMVGGV-28	1	699.4222	Yes	Yes	Yes
VGSNKGAI	1	727.4097	Yes	Yes	Yes
IGLMVGGV	1	727.4171	Yes	Yes	Yes
GSNKGAII and SNKGAIIG	1	741.4254	Yes	Yes	Yes
IIGLMVGG	1	741.4328	Yes	Yes	Yes
HQKLVF	1	753.4406	Yes	Yes	Yes
AEFRHD*	1	756.3424	Yes	Yes	Yes
GSNKGAIIG	1	798.4468	Yes	Yes	Yes
VGSNKGAII	1	840.4938	Yes	Yes	Yes
IIGLMVGGV	1	840.5012	Yes	Yes	Yes
SNKGAIIGL	1	854.5094	Yes	No	No
KGAIIGLMV-NH_3	1	866.5168	Yes	Yes	No
KGAIIGLMV and AIIGLMVGGV-28	1	883.5434	Yes	Yes	Yes
GSNKGAIIGL	1	911.5309	Yes	No	No
AIIGLMVGGV	1	911.5383	Yes	No	No
NKGAIIGLMV and KGAIIGLMVGG	1	997.5863	Yes	No	No

All b^+ ions with the prefix 'Modified' represent those containing the observed mass loss of 89.2 Da. * Due to instrumental resolution limits peaks highlighted may represent either b_6^+ or an internal A_2EFRHD^+ fragment. ‡ Due to instrumental resolution limits peaks highlighted may represent either b_5^+ or an internal $F_{20}AEDVG$ fragment.

Supplementary Methods

Materials and methods. All reagents were purchased from commercial suppliers and used as received unless otherwise noted. $A\beta_{40}$ and $A\beta_{42}$ (the sequence of $A\beta_{42}$: DAEFRHDSGYEVHHQKLVFFAEDVGSNKGAIIGLMVGGVVIA) were purchased from Anaspec Inc. (Fremont, CA, USA). Trace metals were removed from buffers and solutions used in Aβ experiments by treating with Chelex overnight (Sigma-Aldrich, St. Louis, MO, USA). Optical spectra were recorded on an Agilent 8453 UV-visible spectrophotometer. Absorbance values for biological assays, including cell viability and antioxidant assays, were measured on a Molecular Devices SpectraMax 190 microplate reader (Sunnyvale, CA, USA). ^{1}H and ^{13}C NMR spectra were recorded using a 400 MHz Agilent NMR spectrometer.

Preparation of 4-nitro-*N*-(pyridin-2-ylmethyl)aniline. 4-Nitro-*N*-(pyridin-2-ylmethyl)aniline was synthesized using previously reported methods with modifications[7]. To a flame-dried flask equipped with a stir bar and a reflux condenser under N_2 (g), 1-fluoro-4-nitrobenzene (231 μL, 2.2 mmol) and *N*,*N*-diisopropylethylamine (836 μL, 4.8 mmol) were added to DMF (25 mL) followed by the introduction of 2-(aminomethyl)pyridine (247 μL, 2.4 mmol) at room temperature. The resulting solution was heated to 70 °C. After 24 h, the brown solution was added to water (75 mL) and extracted with EtOAc (3 x 75 mL). The organic layers were washed with water (2 x 75 mL) and brine (75 mL), dried with $MgSO_4$, and concentrated under vacuum. The resulting residue was then purified on a silica column (25% to 100% EtOAc in hexanes) yielding a yellow solid (0.29 g, 58%) [TLC (EtOAc:hexanes = 50:50 (v/v)): R_f = 0.25]. ^{1}H

NMR [400 MHz, CD_2Cl_2, δ (ppm)]: 8.56 (d, 1H, *J* = 8 Hz), 8.09 (d, 2H, *J* = 8 Hz), 7.71 (t, 1H, *J* = 8 Hz), 7.30 (d, 1H, *J* = 8 Hz), 7.25 (d, 1H, *J* = 4 Hz), 6.68 (d, 2 H, *J* = 8 Hz), 6.04 (s, 1H), 4.53 (d, 2H, *J* = 8 Hz). ^{13}C NMR [100 MHz, CD_2Cl_2, δ (ppm)]: 156.2, 153.5, 149.5, 138.5, 137.2, 126.6, 123.0, 122.1, 111.8, 48.2.

Preparation of 1. The compound **1** was purchased from Ryan Scientific (Mt. Pleasant, SC, USA) and recrystallized from CH_2Cl_2/hexanes four times. ^{1}H NMR [400 MHz, $(CD_3)_2SO$, δ (ppm)]: 8.49 (d, 1H, *J* = 4 Hz), 7.70 (t, 1H, *J* = 4 Hz), 7.35 (d, 1H, *J* = 4 Hz), 7.22 (t, 1H, *J* = 4 Hz), 6.36 (m, 4H), 5.46 (s, 1H), 4.23 (m, 4H). ^{13}C NMR [100 MHz, CD_2Cl_2, δ (ppm)]: 159.58, 149.50, 141.44, 138.65, 136.75, 122.30, 121.99, 116.85, 114.88, 50.69. ESI(+)MS (*m*/z): $[M+H]^+$ Calcd. for $C_{12}H_{14}N_3$, 200.12; found, 200.03.

Additionally, **1** was also synthesized by adapting previously reported methods[8] to reduce 4-nitro-*N*-(pyridin-2-ylmethyl)aniline. To a solution of 4-nitro-*N*-(pyridin-2-ylmethyl)aniline (0.52 g, 2.3 mmol) and *tris*(acetylacetonato)iron(III) (0.024 g, 3 mol%) in ethanol (20 mL) in a round-bottom flask equipped with a stir bar and a reflux condenser, hydrazine hydrate (581 μL, 11 mmol) was added. The solution was then heated under reflux for 2 h and additional 4 equivalents of hydrazine hydrate were introduced. The mixture was allowed to react for an additional 3 h before removing the solvent under vacuum. The resulting brown oil was purified by silica column chromatography (EtOAc (100%) to EtOAc:Et_3N (99%:1%); TLC (EtOAc:Et_3N = 99:1 (v/v)), R_f = 0.20). The HCl salt of the product was then prepared by dissolving in MeOH and adding excess 5 M HCl. The solvent was removed under vacuum and the resulting residue was washed with Et_2O (3 x 5 mL). The residues were dissolved in water (20 mL). The aqueous layer

was washed with Et_2O (3 x 20 mL) and collected. After removing the water under vacuum and recrystallization using MeOH and Et_2O, the product was obtained (pale yellow powder, 0.45 g. 85%). ^{1}H NMR [400 MHz, $(CD_3)_2SO$, δ (ppm)]: 9.59 (s, 1H), 8.59 (d, 1H, J = 4 Hz), 7.90 (t, 1H, J = 4 Hz), 7.59 (m, 2H), 7.05 (d, 2H, J = 8 Hz), 6.67 (d, 2H, J = 8 Hz), 4.43 (s, 2H). ^{13}C NMR [100 MHz, $(CD_3)_2SO$, δ (ppm)]: 156.0, 147.1, 144.6, 142.9, 125.0, 124.6, 124.0, 120.8, 113.0, 44.8. HRMS (m/z): $[M+H]^+$ Calcd. for $C_{12}H_{14}N_3$, 200.1188; found, 200.1190.

Preparation of 2. The compound **2** was purchased from Ryan Scientific and recrystallized from CH_3CN and water three times (off-white powder). ^{1}H NMR [400 MHz, $(CD_3)_2SO$, δ (ppm)]: 8.52 (d, 1H, J = 4 Hz), 7.73 (t, 1H, J = 8 Hz), 7.35 (d, 1H, J = 8 Hz), 7.24 (t, 1H, J = 8 Hz), 6.35 (t, 1H, J = 8 Hz), 5.75 (s, 2H), 5.71 (s, 1H), 4.31 (d, 2H, 4 Hz), 3.61 (s, 6H). ^{13}C NMR [100 MHz, $(CD_3)_2SO$, δ (ppm)]: 161.1, 159.8, 150.2, 148.8, 136.6, 122.0, 121.1, 91.1, 88.6, 54.7, 48.5. HRMS (m/z): $[M+H]^+$ Calcd. for $C_{14}H_{17}N_2O_2$, 245.1290; found, 245.1288.

Preparation of 3. The compound **3** was purchased from Ryan Scientific and was recrystallized from hot hexanes and washed 5x with cold hexanes (yellow powder). ^{1}H NMR [400 MHz, $(CD_3)_2SO$, δ (ppm)]: 8.29 (d, 1H, J = 8 Hz), 8.00 (d, 1H, J = 8 Hz), 7.93 (d, 1H, J = 8 Hz), 7.74 (t, 1H, J = 8 Hz), 7.56 (m, 2H), 6.57 (m, 4H), 5.91 (t, 1H, J = 4 Hz), 4.47 (d, 2H, J = 8 Hz), 2.67 (s, 6H). ^{13}C NMR [100 MHz, CD_2Cl_2, δ (ppm)]: 159.9, 148.2, 144.8, 141.0, 136.9, 130.0, 129.4, 128.2, 127.9, 126.6, 120.5, 116.1, 114.7, 51.2, 42.39. HRMS (m/z): $[M+H]^+$ Calcd for $C_{18}H_{20}N_3$, 278.1657, found, 278.1656.

Preparation of 4. The compound **4** was purchased from Ukrorgsyntez (Ukraine) and washed with hexanes with one drop of CH_2Cl_2 once and hexanes three or four times (dark brown powder). ^{1}H NMR [400 MHz, $(CD_3)_2SO$, δ (ppm)]: 10.65 (s, 1H), 6.60 (m, 4H), 5.91 (s, 2H), 5.09 (s, 1H), 4.07 (d, 2H, J = 8 Hz), 2.70 (s, 6H). ^{13}C NMR [100 MHz, CD_2Cl_2, δ (ppm)]: 145.3, 140.9, 130.8, 117.6, 115.9, 115.2, 108.7, 106.3, 43.20, 42.27. HRMS (m/z): $[M+H]^+$ Calcd. for $C_{13}H_{18}N_3$, 216.1501; found, 216.1502.

Supplementary References

1. Beck, M. W. *et al.* A rationally designed small molecule for identifying an *in vivo* link between metal–amyloid-β complexes and the pathogenesis of Alzheimer's disease. *Chem. Sci.* **6**, 1879–1886 (2015).
2. Stadtman, E. R. & Levine, R. L. Protein oxidation. *Ann. N. Y. Acad. Sci.* **899**, 191-208 (2000).
3. Inoue, K., Garner, C., Ackermann, B. L., Oe, T. & Blair, I. A. Liquid chromatography/tandem mass spectrometry characterization of oxidized amyloid beta peptides as potential biomarkers of Alzheimer's disease. *Rapid Commun. Mass Spectrom.* **20**, 911-918 (2006).
4. Uchida, K. Histidine and lysine as targets of oxidative modification. *Amino Acids* **25**, 249-257 (2003).
5. Ruotolo, B. T.; Benesch, J. L. P.; Sandercock, A. M.; Hyung, S.-J.; Robinson, C. V. Ion mobility–mass spectrometry analysis of large protein complexes. *Nat. Protoc.* **3**, 1139-1152 (2008).

6. Bush, M. F.; Hall, Z.; Giles, K.; Hoyes, J.; Robinson, C. V.; Ruotolo, B. T. Collision cross sections of proteins and their complexes: a calibration framework and database for gas-phase structural biology. *Anal. Chem.* **82**, 9557−9565 (2010).

7. Jones, C. K. *et al*. Discovery, synthesis, and structure–activity relationship development of a series of *N*-4-(2,5-dioxopyrrolidin-1-yl)phenylpicolinamides (VU0400195, ML182): characterization of a novel positive allosteric modulator of the metabotropic glutamate receptor 4 (mGlu4) with oral efficacy in an antiparkinsonian animal model. *J. Med. Chem.* **54**, 7639−7647 (2011).

8. Sharma, U. *et al.* Phosphane-free green protocol for selective nitro reduction with an iron-based catalyst. *Chem. Eur. J.* **17**, 5903−5907 (2011).